Rotating Spiral Edge Flames in von Karman Swirling Flows

V. Nayagam[1] and F. A. Williams[2]

[1]*National Center for Microgravity Research, NASA Glenn Research Center, Cleveland, Ohio 44135*
[2]*MAE Department, University of California, San Diego, La Jolla, California 92093*

(Received 1 September 1999)

Experimental observations of rotating spiral flame edges formed during near-limit combustion of a downward-facing, polymethylmethacrylate disk spinning in quiescent air are reported. These flames exhibit similarities to patterns commonly found in quiescent excitable media. The tail rotates rigidly while the tip executes a compound, meandering motion sometimes observed in Belousov-Zhabotinskii reactions. A model assuming a rigid-body rotation with a constant speed of propagation relative to the swirling gas flow generated by the spinning disk predicts the observed spiral shapes well.

PACS numbers: 82.40.Py, 47.54.+r, 47.70.Fw, 82.40.Ck

Rotating spiral wave patterns are observed in nature under a variety of situations, including, for example, the propagation of electrical pulses in cardiac muscles [1], slime-mold amoeba aggregation [2], and chemical-reaction fronts in premixed combustion [3]. The common feature among these diverse systems is that they all are supported by an underlying "excitable medium," a term that describes spatially extended, quiescent, and stable matter that can support wave propagation when exited beyond a threshold level, such as certain biological tissues and chemically reactive mixtures (solids, gases, or liquids). Over the past few decades, a prodigious amount of literature has been accumulated in this interdisciplinary area of research, primarily by biologists, chemists, physicists, and mathematicians. Although wave propagation, pattern formation, and reaction-front instabilities historically have been major subjects in the field of combustion [4], very few observations of spiral flame rotations have been reported in the literature thus far [3]. To the best of our knowledge, even these few observations have been limited to premixed flames, in which fuel and oxidizer initially have been intimately mixed at the molecular level, and differential diffusion among various species and heat, characterized by the Lewis number, plays a critical role.

We report, for the first time, observations of rotating spiral flame edges in a diffusion-flame system created by the combustion of a spinning solid polymethylmethacrylate disk in air, a system in which the two reactants initially are unmixed and mix in the course of the combustion process, contrary to premixed flames. Remarkably, the dynamics of these spiral flame edges exhibit a number of similarities to the rotating spiral waves observed earlier in quiescent, excitable media, though the underlying mechanisms are quite different. In particular, the medium is not quiescent but instead is a nonuniformly swirling gas flow. It is well known that there are conditions under which spiral wave patterns, once created in the Belousov-Zhabotinskii (BZ) reaction media, execute a complex rotational behavior [5]. The tail of the spiral rotates as a rigid body while the tip exhibits a "meandering" motion around an inner core region. The meandering is believed to originate from a supercritical Hopf bifurcation that introduces a secondary tip rotational frequency different from the overall tail rotational frequency. Depending on whether the difference between these two frequencies is positive or negative, the tip follows approximately a hypocycloid or an epicycloid path [5]. The exact physical mechanism that causes the meandering motion is still not well understood, although it is linked to the basic parameters of the excitable medium [6]. In the present study, propagating spiral-shaped flame edges formed by local extinction of a diffusion-flame sheet are observed to exhibit both the rigid-body rotation in the tail portion of the flame and meandering at the tip.

Experiments were conducted using a 7 in. diameter, 1/2 in. thick polymethylmethacrylate (PMMA) disk mounted horizontally on an aluminum back plate driven by a stepper motor, with the disk facing downward burning in air. The rotation of the disk generates a flow toward the disk by a viscous pumping action, called the von Karman swirling boundary-layer flow since the mathematical description of this flow was first provided by von Karman [7]. Video images of the flame are obtained using a high-speed intensified-array camera at 250 frames per second. Steadily burning diffusion flames or transient flames that last several seconds are observed depending on the duration of the ignition process. The transient flames lasted for time periods on the order of 15 to 20 s and were observed between rotational speeds of 2 and 20 rps. They took two distinct geometrical configurations. In the first, a flame disk of finite radius, formed initially, shrinks in time at well-defined speeds while maintaining circular symmetry until complete flame extinction occurs as described elsewhere [8]. In the second, an initially circular flame disk breaks symmetry and undergoes transition into a rotating spiral-shaped flame before extinction as described here.

Figure 1 shows a typical sequence of flame spirals at time intervals of 1/30 s for the fuel-disk rotational velocity of 8 rps in the clockwise direction. With the disk rotating clockwise, the flame spirals rotate in the

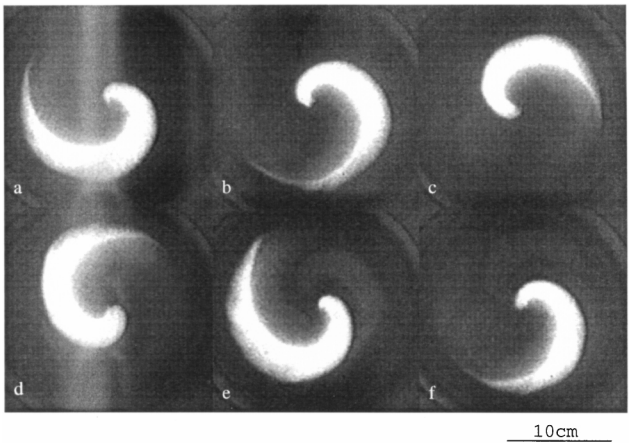

FIG. 1. Typical images of spiral flames shown at 1/30 s intervals; the fuel disk rotates clockwise at 8 rps.

counterclockwise direction at a rate of approximately 5 rps against the local flow. The leading edge of the spiral has a higher image intensity, indicating enhanced reaction rates. In the trailing portion of the flame, the intensity slowly decays to zero. The width of the flame decreases as the distance from the center increases. Once the flame sweeps past a particular point, fuel and oxygen diffuse back and reestablish a flammable layer at that location, into which the leading edge of the spiral flame can propagate when it arrives again, since the diffusion time is short compared with the rotational period. Since the fuel disk continually loses heat to the interior, the observed spiral flame movements are not truly steady, and the overall process is only quasistationary. In general, two distinct modes of spiral flame propagation can be identified, namely, a "rigid-body" rotation mode in which the pattern remains fixed in an appropriate uniformly rotating frame and a "ratcheting" rotation where the spiral accelerates, slows down, and then accelerates again. Figure 2 shows representative results for these two modes of flame rotation, exhibiting leading-edge shapes at 0.024 s intervals. The steady progression of the rigid-body mode and the pauses during the ratcheting mode are evident here. Just prior to extinction, most of the spirals tend to exhibit the ratcheting mode, with rotation periods slightly larger than those of the rigid-body mode. Small portions of the tail sometimes break off and quickly extinguish toward the end of a spiral life cycle. Over the range of rotational speeds investigated, multiarmed spirals were never seen.

Figures 3(a) and 3(b) show the time-series maps of the image intensity and the corresponding Fourier spectra measured at two different points, one located at the center of the disk (solid curves) and the other 3.25 cm away from the center, near the tail of the spiral (dashed curves), for the initial 2 s following ignition at a disk rotational speed of 10 rps. Near the tail there is a periodic behavior with a single dominant frequency at 5.0 Hz, while at the center the motion is less regular, reflecting nose meandering, and the dominant frequency is 10.0 Hz, approximately twice that of the tail. In Fig. 3(a), the width of each spike in the intensity, which corresponds to the flame width, decreases with time, understandable because as time increases the continuous heat loss to the interior causes the flame to become weaker and therefore narrower. Time series of flame intensity for later periods show that the spiral rotation changes to the ratcheting mode, and the Fourier spectrum becomes more complex, with higher-order frequencies. Figure 4 shows the track of the spiral tail and the tip, defined here as the location of maximum

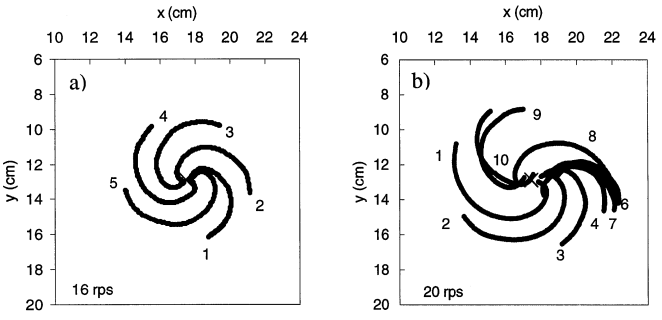

FIG. 2. Successive leading-edge shapes of spiral flames shown at intervals of 0.024 s; the rigid rotation mode is on the left and the ratcheting rotation mode is on the right.

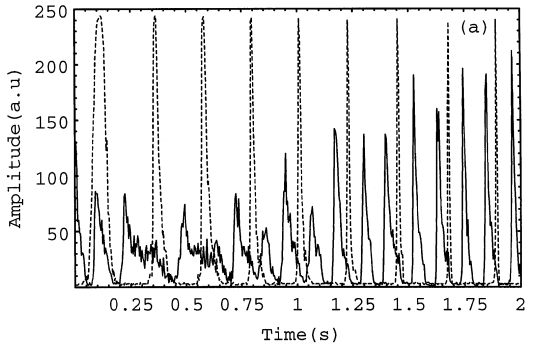

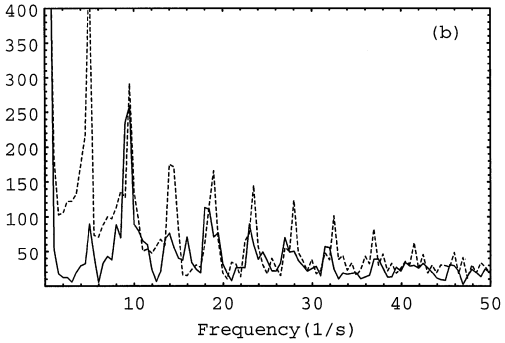

FIG. 3. The time series (a) and its Fourier spectrum (b) of intensity at the center of the disk (solid curves) and at a point 3.25 cm from the center (dashed curves).

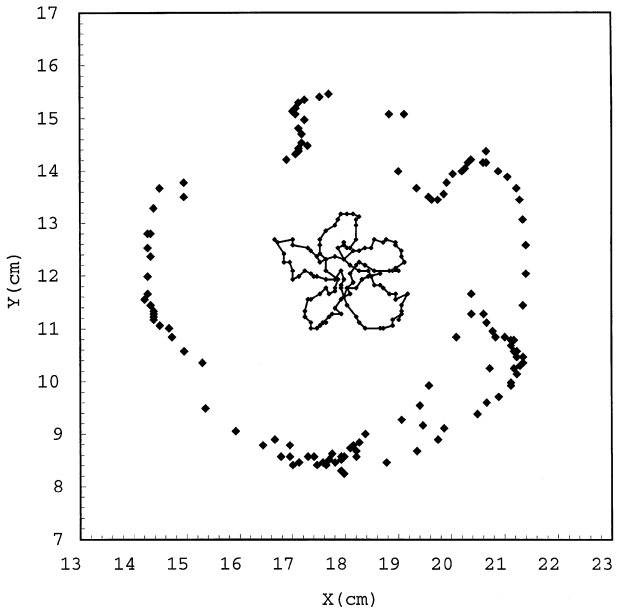

FIG. 4. Location of the spiral tail and the tip for a disk rotational speed of 10 rps, late in the burning history.

curvature, for a time window later than that shown in Fig. 3. This later period, near extinction, was selected because it illustrates the tip motion more clearly. The tail, shown by isolated points at 4 ms intervals, follows a nearly circular path, while the tip meanders. The path of the tail is very circular at earlier periods but fluctuates somewhat in Fig. 4 as the outer parts of the tail begin to extinguish. The tip, shown by connected points at 4 ms intervals, meanders in five arms that resemble a hypocycloid motion, that is, meandering with outward petals [5].

Theoretical descriptions of spiral waves and their meandering have been offered on different levels, ranging from fitting of BZ experimental results on spiral shapes by different spiral functions [9], to empirical descriptions of measurements of BZ meandering [10], to derivations of spiral shapes and meandering and other motions from model equations [11–15]. Two coupled reaction-diffusion equations have provided attractive and versatile models for BZ systems [11,14,15]. Such models are not entirely appropriate for flames because flames experience advection effects as well, particularly in nonuniform flows such as those of the present experiments. Just as front-propagation equations can be derived from the reaction-diffusion equations [11], so can they be derived from the field equations for premixed combustion in nonuniform flows [16,17]. The results show that the fronts propagate locally with respect to the fluid at a constant velocity, the laminar burning velocity, and the front location can be described by an evolution equation for a level surface [18,19]. Since edges of diffusion flames similarly propagate along stoichiometric surfaces at a velocity V with respect to the flow [20,21], we assume that in the present experiments the forward flame edge is a rigidly rotating level curve described in polar coordinates by a function $S(r, \theta) = 0$, enabling a theoretical model for the shape of the leading edge of the spiral flame to be developed.

Since the characteristic time scale of the gas phase is small compared with the solid-phase time scale, a quasi-steady theoretical model is appropriate, in which the leading edge of the flame propagates with respect to the flow induced by the spinning disk at a constant speed V in the stoichiometric plane. We assume that the flow field in the stoichiometric plane is given by the von Karman similarity solutions [7] corresponding to a flat diffusion-flame sheet, namely,

$$\boldsymbol{v} = a\Omega r\boldsymbol{e}_r + b\Omega r\boldsymbol{e}_\theta , \tag{1}$$

where a and b are constant dimensionless velocities evaluated at the flame sheet, Ω is the angular rotational velocity of the fuel disk, and $\boldsymbol{e}_r$ and $\boldsymbol{e}_\theta$ are the unit vectors in the r and θ directions, respectively. The equation of motion of the spiral leading edge is then

$$\boldsymbol{n} \cdot d\boldsymbol{x}/dt = \boldsymbol{v} \cdot \boldsymbol{n} + V , \tag{2}$$

in which $\boldsymbol{n} = \nabla S/|\nabla S|$ is the unit normal to the curve $S = 0$, and $\boldsymbol{n} \cdot d\boldsymbol{x}/dt$ is the speed of motion of the leading-edge curve normal to itself. If the spiral rotates as a rigid body with angular velocity ω, then $d\boldsymbol{x}/dt = \omega r\boldsymbol{e}_\theta$, and, when S is expressed as $S(r, \theta) = \theta - F(r)$, Eq. (2) becomes

$$\omega = b\Omega + a\Omega r dF/dr + V[r^2 + (dF/dr)^2]^{1/2}. \tag{3}$$

In terms of the nondimensional coordinate $\xi = ra\Omega/V$ and function $f(\xi) = F(r)$, Eq. (3) gives

$$df/d\xi = [R\xi - (1 + R^2 - \xi^{-2})^{1/2}]/(1 - \xi^2), \tag{4}$$

where the parameter $R = (b\Omega - \omega)/(a\Omega)$ is the ratio of the tangential component to the radial component of the flow velocity as seen from a coordinate system fixed to the flame edge. When R is large, the flow seen by the flame is essentially a rigid-body rotation, and when R is small it is a primarily radial flow. The magnitude of the flow velocity in a reference frame fixed to the flame front then can be expressed in terms of R and ξ as $V(1 + R^2)^{1/2}\xi$. When $\xi = \xi_c \equiv 1/(1 + R^2)^{1/2}$, the flow velocity is equal to the flame-edge propagation speed V. For $\xi < \xi_c$, the flow velocity is smaller than the edge-flame speed, and steady edge flames cannot exist within this inner core.

Figure 5 shows a plot of spiral edge-flame shapes for three different values of R (0.5, 2, and 9), obtained by integrating Eq. (4) with an arbitrary common starting condition $f(3.7) = 3\pi/4$. The general shapes of the flame edges are independent of the starting conditions. For a smaller value of R, the flame edge turns faster as it approaches ξ_c, and for a larger R the turning is more

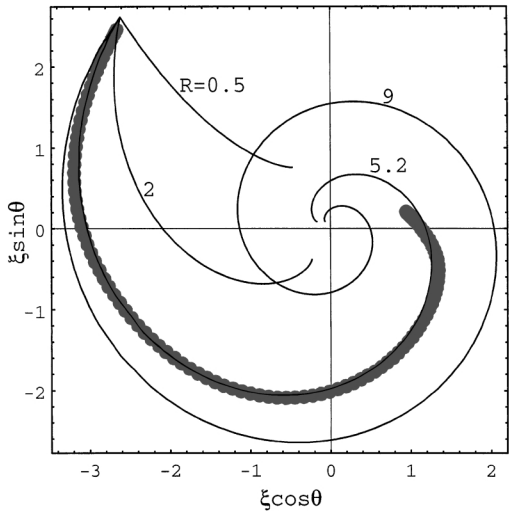

FIG. 5. Theoretical shapes of the leading edge of the flame for different values R (light curves), and comparison of theoretical and experimental shapes of the flame leading edge in one case (heavy curve).

gradual. Also shown in Fig. 5 is a comparison between an experimentally measured flame-edge profile and the theoretical calculations according to Eq. (4). To obtain the best fit, two parameters were varied: the scale for the length $(V/a\Omega)$ which determines the size of the flame, and the shape parameter R which determines the curvature. The experiment had $\Omega = 14$ rps and the measured flame rotational velocity ω of -5.5 rps, the best match being achieved for $V/a\Omega = 0.75$ and $R = 5.2$. The von Karman swirling flows [22] relate a and b which are functions of the mass transfer number B and the Prandtl number Pr. For air (Pr $= 0.7$), a varies from 0.16 to 0.06, and b from 0.70 to 0.07 as B is varied from 0.15 to 1.0. The combination of a and b that gives $R = 5.2$ corresponds to V of 13 cm/s and $B \sim 0.3$, reasonable for the current experimental condition because of the large amount of heat loss to the interior. Further investigations are needed to identify tip-meandering mechanisms.

This work was supported by the Microgravity Science Division of the NASA Headquarters. Stephen Hostler helped with the experiments and data reduction.

[1] J. M. Davidenko, A. V. Pertsov, R. Salamonz, W. Baxter, and J. Jalife, Nature (London) **355**, 349 (1992).
[2] G. Gerish, Naturwissenschaften **58**, 420 (1983).
[3] M. Gorman, F. Hamill, M. el-Hamdi, and K. Robbins, Combust. Sci. Technol. **98**, 25 (1994); H. Pearlman and P. Ronney, Phys. Fluids **6**, 4009 (1994); M. Gorman, B. Pearson, M. el-Hamdi, and K. A. Robbins, Phys. Rev. Lett. **76**, 228 (1996); G. H. Gunaratne, M. el-Hamdi, M. Gorman, and K. A. Robbins, Mod. Phys. Lett. B **10**, 1379 (1996); A. Palacios, G. H. Gunaratne, M. Gorman, and K. A. Robbins, Chaos **7**, 463 (1997); H. Pearlman, Combust. Flame **109**, 382 (1997).
[4] F. A. Williams, *Combustion Theory* (Addison-Wesley, Redwood City, CA, 1985); *Non-Steady Propagating Flames*, edited by G. H. Markstein (MacMillan, New York, 1964).
[5] G. Li, Q. Ouyang, V. Petrov, and H. Swinney, Phys. Rev. Lett. **77**, 2105 (1996).
[6] V. Hakim and A. Karma, Phys. Rev. Lett. **79**, 665 (1997).
[7] Th. von Karman, Z. Angew. Math. Mech. **1**, 233 (1921).
[8] V. Nayagam and F. A. Williams, "Symmetrical Edge Flames in von Karman Swirling Flows" (to be published).
[9] S. C. Müller, T. Plesser, and B. Hess, Physica (Amsterdam) **24D**, 87 (1987).
[10] G. S. Skinner and H. L. Swinney, Physica (Amsterdam) **48D**, 1 (1991).
[11] J. J. Tyson and J. P. Keener, Physica (Amsterdam) **32D**, 327 (1988).
[12] E. Meron, Phys. Rev. Lett. **63**, 684 (1989).
[13] E. Lugosi, Physica (Amsterdam) **40D**, 331 (1989).
[14] W. Jahnke, W. E. Skaggs, and A. T. Winfree, J. Phys. Chem. **93**, 740 (1989).
[15] D. M. Goldschmidt, V. S. Zykov, and S. C. Müller, Phys. Rev. Lett. **80**, 5220 (1998).
[16] G. I. Sivashinsky, Acta Astronaut. **3**, 883 (1976).
[17] N. Peters and F. A. Williams, in *Proceedings of the Twenty-Second International Symposium on Combustion* (Combustion Institute, Pittsburgh, PA, 1988), p. 495.
[18] A. R. Kerstein, W. T. Ashurst, and F. A. Williams, Phys. Rev. A **37**, 2728 (1988).
[19] W. J. Sheu and G. I. Sivashinsky, Combust. Flame **84**, 221 (1991).
[20] J. Buckmaster, Physica (Amsterdam) **12D**, 173 (1984).
[21] J. Daou and A. Liñán, Combust. Theory Model. **2**, 449 (1998).
[22] M. D. King, V. Nayagam, and F. A. Williams (to be published).